Int. J. Electron. Commun. (AEÜ) 180 (2024) 155338

Contents lists available at ScienceDirect

Int. J. Electron. Commun. (AEÜ)

journal homepage: www.elsevier.com/locate/aeue

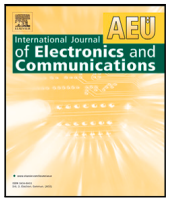

Regular paper

Multimodal planar monopole filtenna for 5G applications

Miquel Ribó [a], Marta Cabedo-Fabrés [b], Lluís Pradell [c,*], Sebastián Blanch [c], Miguel Ferrando-Bataller [b]

[a] La Salle–Universitat Ramon Llull, Barcelona, Spain [1]
[b] Universitat Politècnica de València, Valencia, Spain
[c] Universitat Politècnica de Catalunya, Barcelona, Spain

ARTICLE INFO

Keywords:
Characteristic modes
Coupled monopoles
Even mode
Odd mode
Filtenna
Filtering antenna
Modal analysis
Monopole
Planar antenna
Slotline

ABSTRACT

This paper presents a novel planar filtering antenna (filtenna) with simple layout based on tightly-coupled different-length monopoles. Its design methodology is based on an even-mode/odd-mode decomposition of the monopole currents, and the combination of both modes in a multimodal circuit model that facilitates the design and tuning of the antenna and the accompanying feeding network, since most of the process is performed using fast circuit simulations. The circuit model casts light into the interaction between conducting and radiating modes in the bulk of the antenna, and on how this interaction can be used to propose feedback loops that increase and define the radiation band. Using these modal tools, a filtenna was designed and fabricated to fully cover the new 5G frequency bands (n77, n78 and n79) from 3 to 5 GHz that are currently being adopted by many countries for high-capacity data transmission. It features a 62.9% FWB, dipole-like radiation patterns, good out-of-band rejection up to 10 GHz, and a very good trade-off between design/structural-simplicity and bandwidth.

1. Introduction

The new 5G communication systems require antennas that, in addition to having a stable pattern, good efficiency and low return losses, can perform filtering functions to avoid interference with other nearby frequency systems. A number of 5G frequency bands have been recently assigned to TDD high-capacity data-transmission networks (n77: 3300–4200 MHz; n78: 3300–3800 MHz; and n79: 4400–5000 MHz) [1], and are currently being adopted in Europe, China, Japan, South Korea and USA. To ensure a world-wide coverage of these new services with compact and low-cost systems, it is advisable to use receiving antennas with a wide bandwidth from 3 GHz to 5 GHz. Receiving systems usually perform the antenna and filtering functions separately—filter design is usually performed using microwave circuits or resonant cavities—, but a large number of filtering-antenna (or filtenna) designs with multiple resonant elements can also be found in the literature. By integrating the filtering functions with the antenna structure, the frequency selectivity and fractional bandwidth (FBW) can be optimized and the overall cost and size minimized. Many filtenna structures and design approaches have been proposed in the literature, of which an extensive review can be found in [2]. Bandpass filters in filtennas are frequently designed separately using well-established filter design techniques, implemented using microstrip resonators, and then integrated with the antenna [3–9]. Further integration and improved selectivity are achieved using high-Q surface-integrated waveguide (SIW) filters or cavities, which require via-holes [10–14]. Multilayer structures for filtennas have also been proposed to reduce footprint size, using stacked dielectric resonators (DR) [15], top-hat loaded monopoles [16], microstrip coupled resonators (MCR) [17–19], or stacked SIW cavities [20,21] to synthesize the filtering function.

Concerning the FBW, while filtennas with filters connected in cascade (not embedded in the antenna structure) may exhibit a large FBW (112.2% reported in [4]), multilayer and SIW-based filtennas feature small to moderate FBW, ranging from 2.4% to 61.4%, as reported in [13,15], respectively. The filters can also be designed to support more than one radiation bandwidth, such as the dual-band filtennas reported in [9,13], with FBW values that depend also on the type of filtenna design. Concerning the design approach and fabrication, multilayer and SIW-based filtennas frequently feature a complex structure that requires complex design and simulation procedures to match the behavior of the antenna with that of the embedded filter, as well as involved mask-alignment and layer-attachment procedures.

In this paper a novel design approach for coupled-monopole planar filtennas, based on a multimodal analysis of the antenna structure

* Corresponding author.
E-mail addresses: miquel.ribo@salle.url.edu (M. Ribó), marcafab@dcom.upv.es (M. Cabedo-Fabrés), lluis.pradell@upc.edu (L. Pradell), sebastian.blanch@upc.edu (S. Blanch), mferrand@dcom.upv.es (M. Ferrando-Bataller).
[1] Concerning this work.

https://doi.org/10.1016/j.aeue.2024.155338
Received 13 March 2024; Accepted 10 May 2024
Available online 18 May 2024
1434-8411/© 2024 The Author(s). Published by Elsevier GmbH. This is an open access article under the CC BY-NC-ND license (http://creativecommons.org/licenses/by-nc-nd/4.0/).

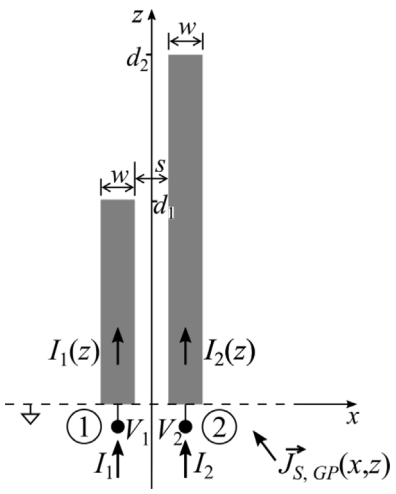

Fig. 1. Two tightly-coupled different-length planar monopoles over a ground plane.

and coupling to the feeding section, is proposed. It seeks to achieve a well-defined, wide bandwidth by integrating very simple radiating elements and the microstrip feed into a multimodal circuit. Coupled monopoles are selected as radiating elements because of their potential wideband behavior whenever they are anti-symmetrically fed with an appropriate microstrip coupled-line structure. The use of coupled radiating elements of different lengths increases the fractional bandwidth and allows a precise control of the pass band. In contrast with previous filtenna designs, a multimodal circuit model is proposed to analyze in a unified manner the conduction behavior of the feeding network (and part of the antenna) with the radiating behavior of the antenna, thus providing a methodology for the filtenna design and optimization. From a circuit (i.e. based on voltages and currents) point of view, coupled-line (or multimodal) circuits can be analyzed using general coupled-mode theory [22,23], wherein circuit-to-modal transformer networks can be used to transform the physical voltages and currents into their equivalent modal ones. Alternatively, they can be analyzed by means of particular multimodal circuit models (for instance [24–27]) that, although more specific than those of [22], are simpler and, therefore, provide better insight into the circuit modal behavior. These analyses can be applied to a variety of circuit configurations based on coupled-line sections such as filters, directional couplers, phase shifters and baluns, and will be extended in this paper to radiating elements.

The novelty of the article lies not in the specific antenna design, but rather in the comparison of different resonance-analysis methodologies. The characteristic-mode methodology is compared with the classical modal analysis used in microwave circuit theory. Both approaches yield equivalent results. However, the circuit methodology is much more efficient from the computational point of view, when dealing with coupled lines and the classical decomposition into electrically and magnetically symmetric structures. The developed methods can be applied to more complex cases, involving a greater number of resonances. Furthermore, the study demonstrates that the radiation patterns are typical of a monopole antenna, but with an exceptionally broad bandwidth.

2. Modal analysis of two tightly-coupled different-length monopoles

The decomposition of antenna currents into even-mode/odd-mode (or symmetric-mode/anti-symmetric-mode) configurations is a widely employed technique for analyzing the behavior of traditional folded dipoles. In this study, this approach is extended to a more complex scenario, which entails tightly-coupled yet physically unconnected planar monopoles of different lengths.

Consider the two tightly-coupled different-length planar monopoles of Fig. 1 on one side of a dielectric substrate, with the associated ground plane on the other side (for $z < 0$). For $z < d_1$ the currents on the monopole strips ($I_1(z)$ and $I_2(z)$) and ground plane ($\mathbf{J}_{S,GP}(x,z)$) can be *mathematically* decomposed as a part or *mode* symmetric with respect to z and a part or *mode* anti-symmetric with respect to z. The symmetric (or even) mode will have currents in the strips flowing in the same direction, $I_R(z)/2$ in either strip, and currents in the ground plane flowing along the ground-plane edge ($z = 0$) in opposite directions, $I_R(|x|)/2$ on either side: it will be a radiating mode [Fig. 2(a)]. The current $I_2(z)$ for $z > d_1$ will also contribute to the radiation, and so it can be re-labeled as $I_R(z)$. Since the radiation processes cannot be easily described from a circuit point of view, this mode can only be modeled as a *black-box* two-port, with scattering parameters S_R to be found by electromagnetic simulation. Port one of the two-port (1_R) is at the excitation plane at $z = 0$, and port 2 (2_R) is at $z = d_1$, where a complex interaction with the anti-symmetric mode may occur. The anti-symmetric (or odd) mode will have currents, $I_S(z)$, flowing in opposite directions, so their radiation will cancel out: it will be a conducting, slotline, mode [Fig. 2(b)]. The slotline mode requires a transverse voltage drop between conductors, and therefore it cannot be extended beyond $z = d_1$. This mode can easily be modeled by an ideal transmission line. More currents may be present in the system due to antenna (to-be-defined) feeding circuit, flowing on microstrip/coupled-microstrip transmission lines patterned over the ground plane for $z < 0$. These currents will contribute negligibly to the radiation, since any current on a strip will be *mirrored* by an opposite-direction current in the back ground plane, and so they can be ignored when analyzing the basic antenna behavior. For $0 \le z \le d_1$,

$$I_1(z) = \frac{I_R(z)}{2} + I_S(z) \tag{1}$$

$$I_2(z) = \frac{I_R(z)}{2} - I_S(z) \tag{2}$$

In general, modal interactions take place at any circuit transition or asymmetry. Therefore, the radiating mode [Fig. 2(a)] and the slotline mode [Fig. 2(b)] may interact at $z = d_1$. Consider the currents of both modes at $z = d_1$, as shown in Fig. 1. They meet the obvious conditions at $z = d_1$,

$$\begin{aligned} &I_1(d_1) = 0 \Rightarrow \\ &\frac{I_R(d_1)}{2} + I_S(d_1) = \frac{I_{R2}}{2} - I_{S2} = 0 \Rightarrow \\ &I_{R2} = 2I_{S2} \end{aligned} \tag{3}$$

and

$$\begin{aligned} &I_2(d_1^-) = I_2(d_1^+) \Rightarrow \\ &\frac{I_R(d_1)}{2} - I_S(d_1) = I_R(d_1) \Rightarrow \\ &\frac{I_{R2}}{2} + I_{S2} = I_{R2} \Rightarrow \\ &I_{R2} = 2I_{S2}\ . \end{aligned} \tag{4}$$

The resulting relationship $I_{R2} = 2I_{S2}$ between modal currents can be modeled by means of an ideal transformer connecting the radiating-mode model to the slotline-mode model, as shown in Fig. 3, which constitutes a complete *multimodal* circuit model, with *modal* ports (ports 1_R and 1_S in Fig. 2) instead of the *uncoupled circuit* ports (ports 1 and 2 of Fig. 1), for the coupled monopoles of Fig. 1. This model is multimodal since it confines the excitation of either mode present in the antenna into a different port. Thus, situations wherein the antenna feeding scheme differently affects either mode can be easily taken into account. It should be noted that the slotline mode is not open-circuited at the end of the coupled-strip section, but excites (and is excited by) the radiation mode.

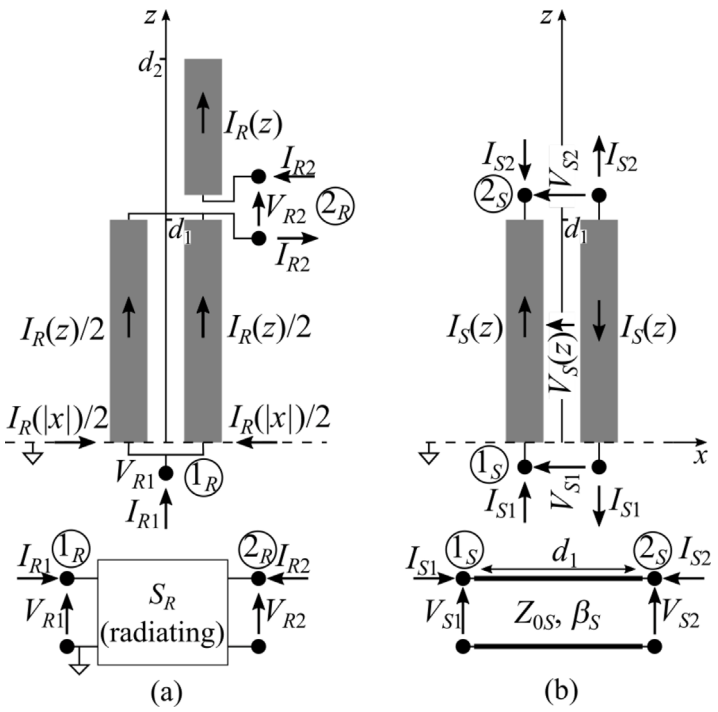

Fig. 2. Current and voltage distributions (above) and equivalent circuit models (below) for the radiating and slotline modes. (a) Radiating mode. (b) Slotline mode.

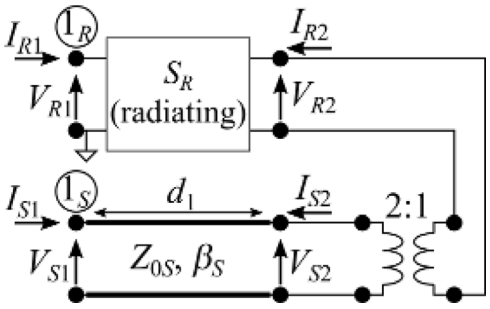

Fig. 3. Multimodal circuit model (with modal ports) for the tightly-coupled different-length monopoles of Fig. 1.

It should be emphasized that the radiating and slotline modes in Fig. 2 were defined on purely mathematical grounds, and will accurately-enough describe the reality as far as (i) a *black-box* model (two-port S_R) for the symmetric/even/radiating mode can be obtained through an electromagnetic simulation (i.e. an electromagnetic simulation of the antenna can be performed that keeps currents on both dipoles for $z < d_1$ of equal, or similar, magnitude and direction), and (ii) an ideal transmission line is an accurate model for the anti-symmetric/odd/slotline mode (i.e. s is small in terms of wavelength). To fulfill condition (i), in the electromagnetic simulation of the radiating mode, the two monopole strips should be connected at $z = 0$ and $z = d_1$ by narrow *horizontal* strips to keep both conductors at the same transverse potential and hinder the apparition of spurious transmission-line-like currents.

3. Mathematical modes and characteristic modes

A fast and direct approach to obtain a modal decomposition of the currents of an antenna by electromagnetic simulation is to compute the characteristic modes of the structure [28–30]. However, the symmetric

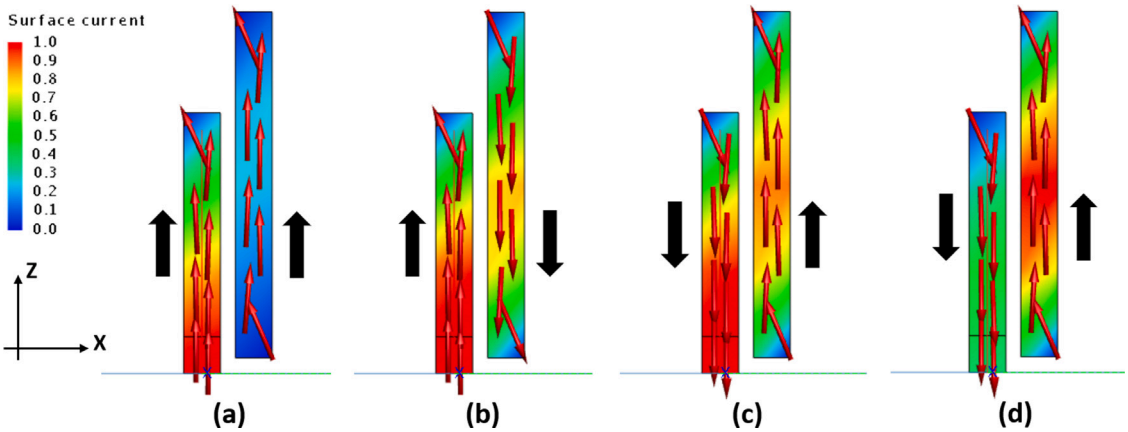

Fig. 4. Normalized characteristic current of the first two modes of two tightly-coupled different-length monopoles at first (4.6 GHz) and second (7.6 GHz) resonances. (a) Mode J_1 at 4.6 GHz. (b) Mode J_1 at 7.6 GHz. (c) Mode J_2 at 4.6 GHz. (d) Mode J_2 at 7.6 GHz.

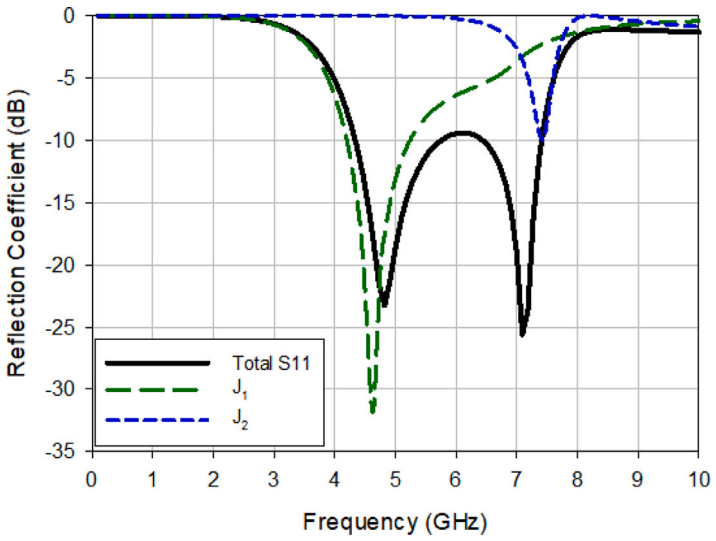

Fig. 5. Contribution of modal reflection coefficients to the total reflection coefficient of two tightly-coupled different-length monopoles when the shorted monopole is excited and the longest is in open circuit-condition.

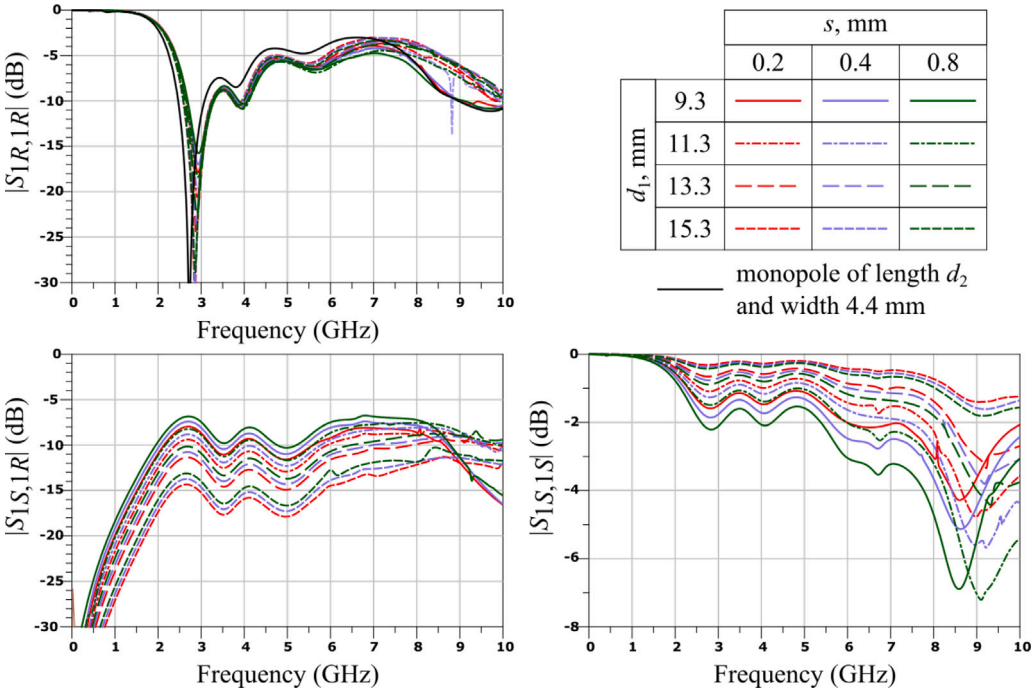

Fig. 6. S parameters for the multimodal model of Fig. 3 for several dimension choices of the shorter monopole length (d_1) and separation between monopoles (s), with fixed strip width $w = 2$ mm and fixed longer monopole length $d_2 = 19.1$ mm. With reference to Fig. 3, $S_{1R,1R}$ is the S_{11} (reflection) parameter of the radiating mode (port 1_R), $S_{1S,1R}$ is the transmission parameter between the radiating mode (port 1_R) and the slotline mode (port 1_S), and $S_{1S,1S}$ is the S_{11} (reflection) parameter of the slotline mode (port 1_S). The $S_{1R,1R}$ parameter is compared with the input reflection coefficient of a wide monopole of length d_2 and strip width 4.4 mm ($2w + s$ for $s = 0.4$ mm).

(radiating) and anti-symmetric (slotline) modes used in the previous Section 2 do not precisely correspond to these characteristic modes. The latter, generally speaking, do not keep the symmetry with respect to z for $z < d_1$, and evolve from radiating modes to slotline modes as the operation frequency moves away from the mode resonance. Take, for instance, the simple example antenna of Fig. 4: two tightly-coupled different-length monopoles of *arbitrary* lengths $d_1 = 14.1$ mm and $d_2 = 20.4$ mm, over a perpendicular ground plane for simulation simplicity. The characteristic modes of this structure were numerically computed using the electromagnetic simulator FEKO. The contribution of the first two radiating modes of the structure (modes J_1 and J_2) to the total S_{11} of the antenna is shown in Fig. 5.

The evolution of the normalized modal currents of these first two characteristic modes depicted in Fig. 4 confirms that characteristic

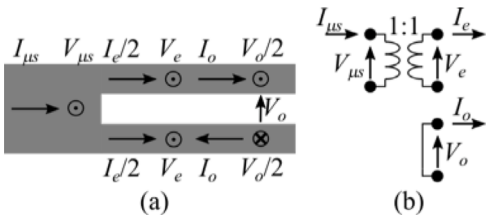

Fig. 7. (a) Microstrip to coupled-microstrip transition (back-side ground plane not shown). (b) Multimodal model.

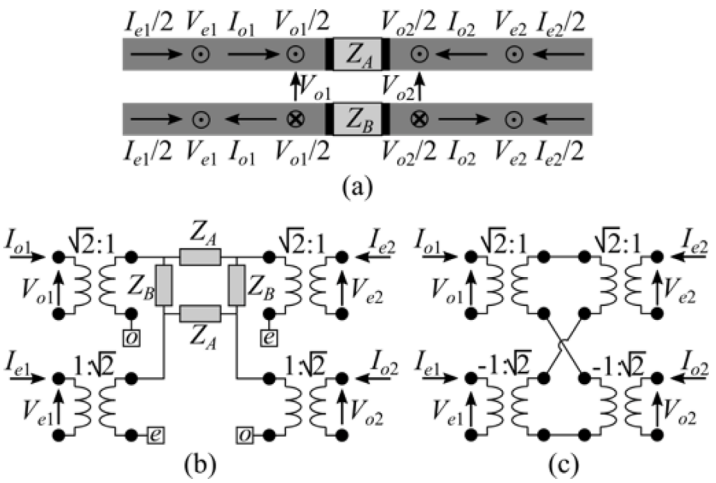

Fig. 8. (a) Asymmetric series impedances in a coupled-microstrip transmission line (back-side ground plane not shown). (b) Multimodal model. (c) Multimodal model for $Z_A = 0, Z_B \to \infty$.

modes do not exhibit the current symmetries forced in the *mathematical* modes defined in Section 2, revealing the coupling effects between the two radiating elements at different frequencies. Only for the case $d_1 = d_2$ (which is not suited for our purpose) there is a more direct relationship between these *mathematical* modes and the first two characteristic modes, whose currents tend to have the desired symmetric/anti-symmetric behavior in a wide frequency range.

However, a characteristic-mode analysis can be a guiding principle to assess the filtenna capabilities of generic antenna configurations based on coupled elements: from the characteristic-mode analysis of antennas such that of Fig. 4 with different monopole open-circuiting/short-circuiting schemes, it can be concluded that a configuration with the long open-circuited element is the one exhibiting a widest well-defined bandwidth. In fact, the antenna of Fig. 1 is a generalization of the antenna-type of Fig. 4 in a planar context, which allows more degrees of freedom in the design procedure (for instance, as will be seen, the open circuit at the beginning of the longest element will be transformed into a gap in a coupled microstrip line that can recede into the antenna feeding network) and ease fabrication.

4. Modal behavior in tightly-coupled different-length monopoles

The behavior of the multimodal model of Fig. 3 will depend largely on the behavior of the radiating mode, which must be computed by means of electromagnetic simulation. Therefore the modal behavior of the multimodal model of Fig. 3 must be analyzed by means of a mixed circuit-electromagnetic parametric study. The substrate used in this work was a Rogers RO4003 substrate with dielectric thickness $h = 0.81$ mm, relative dielectric permittivity $\epsilon_R = 3.55$, and copper-metallization thickness $t = 17.5$ μm, and the circuit and electromagnetic simulations were performed using Keysight's simulators ADS, Momentum and EMPro.

The fixed dimensions were $d_2 = 19.1$ mm—length of the longer antenna strip, chosen so that the long monopole have a first S_{11} resonance around 3 GHz, the intended lower band limit—and $w = 2$ mm, and several values of d_1 (length of the shorter antenna strip) and s (separation) were parametrically analyzed. The S parameters for the multimodal model of Fig. 3 are shown in Fig. 6—port 1_R with reference impedance 50 Ω, and port 1_S with reference impedance Z_{0S}, the characteristic impedance of the associated slotline—and compared with the input reflection coefficient of a wide monopole of length d_2 and strip width 4.4 mm ($2w + s$ for $s = 0.4$ mm).

For frequencies wherein the upper part of the long monopole, of length $d_2 - d_1$, is short in terms of wavelength, it is difficult to inject currents at port 2_R of the radiating mode due to the proximity of the

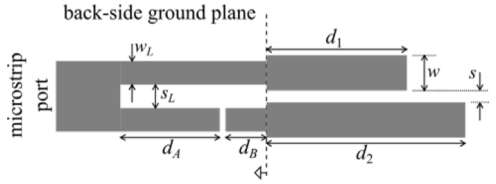

Fig. 9. Antenna and feeding network structure for a planar filtering antenna.

zero current condition at $z = d_2$ and its sinusoidal variation along the strip. Therefore, it is reasonable that $S_{1R,1R}$ show little variation with d_1 in this frequency range since the power transfer to port 2_R is low. Taking this into account, the behavior of $S_{1S,1R}$ and $S_{1S,1S}$ is also coherent: the larger is d_1, the more difficult it is to inject current at port 2_R, and therefore the lower is the power transfer to port 1_R—therefore $|S_{1S,1R}|$ decreases, thus decreasing the coupling between ports 1_R and 1_S—and the higher is the input impedance at the port 1_S—therefore $|S_{1S,1S}|$ increases. As d_1 increases to match d_2 the conducting and radiating modes get increasingly uncoupled. Concerning the monopole separation s, the results might seem counter-intuitive: the closer the monopoles, the lesser the coupling between modes. This is due to the fact that the S parameters of the radiating mode are rather independent of the separation s, which is small as compared to the wavelength, due to the equal orientation of currents in either monopole for the radiating mode for $z < d_1$. The observed variation is due to the fact that Z_{0S}, to which port 1_S is referenced, increases with s. Therefore, by increasing s the reference port impedance is made closer to the inner impedance of port 2_R, which facilitates the power injection into port 2_R, and its transfer to port 1_R. Finally, a comparison with the behavior of a single monopole of length d_2 and width $2w+s$ (for $s = 0.4$ mm) shows than, as seen from port 1_R, the structure behaves basically as a single monopole, quite independently of the behavior of port 1_S. To increase the effect of port 1_S on the radiation it is necessary to integrate the slotline mode into a feedback loop, as that proposed in Section 5 for the designed antenna.

The above results indicate that one possible use of the tightly-coupled different-length monopoles could be as an antenna which excites mainly port 1_R of the radiating element around the first monopole resonance (controlled by the length d_2), where there is a good-enough matching, using port 1_S to control the overall antenna behavior by means of a slotline feedback loop. This feedback loop should be closed by the feeding circuit of the antenna. This feedback network should be implemented using coupled microstrip lines, since their

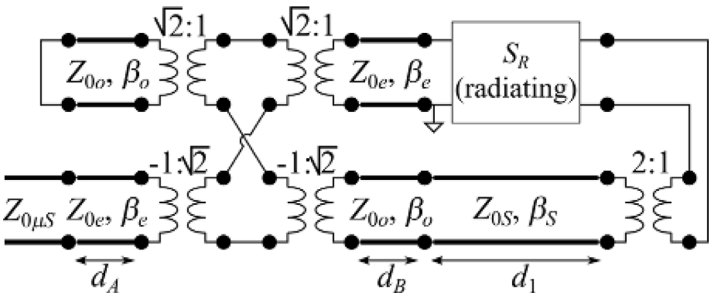

Fig. 10. Multimodal model for the antenna of Fig. 9.

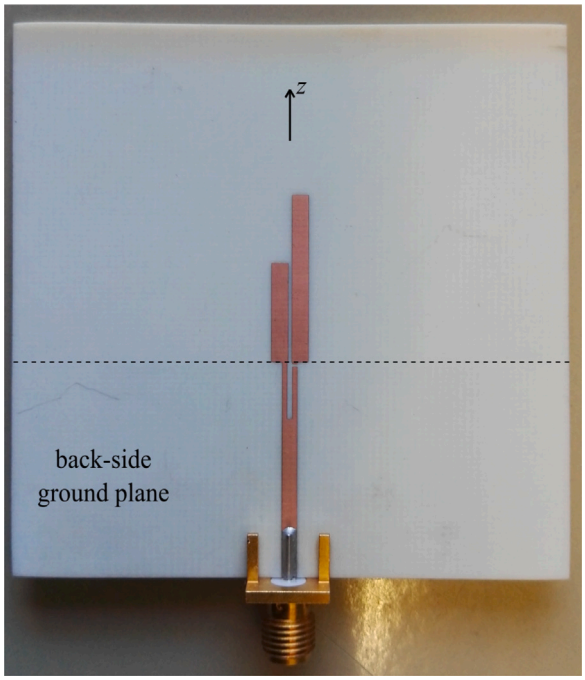

Fig. 11. Top-view picture of the fabricated antenna.

symmetric/even/common mode is compatible with the microstip mode (and hence, with the radiating mode at port 1_R) and their anti-symmetric/odd/differential mode is compatible with the slotline mode. Different feeding circuits will result in different modal couplings at $z = 0$ and, therefore, in different feedback loops and antenna behaviors. In the following section the building blocks for a feeding network resulting in a global filtenna behavior are described.

5. Multimodal model for tightly-coupled planar monopoles fed by coupled-microstrip networks for filtennas

A suitable feeding network for the tightly-coupled monopoles of this work can be obtained by combining a symmetric transition from a microstrip to a coupled-microstrip transmission line [Fig. 7(a)]—it transforms the microstrip mode into the even mode (they have similar voltage and current orientations) and short-circuits the odd mode [Fig. 7(b)]—and the transition formed by two series asymmetric impedances Z_A and Z_B in a coupled-microstrip transmission-line section [Fig. 8(a)]—they cause a modal balance that can be modeled by the multimodal circuit of Fig. 8(b) [27], or Fig. 8(c) when $Z_A = 0$, $Z_B \to \infty$.

With the aforementioned multimodal models, among others, a variety of feeding networks for the tightly-coupled different-length monopoles of Fig. 1(a) can be proposed. They are generally too involved to allow an analytical circuit analysis, but permit fast and versatile circuit optimizations and parametric studies—as opposed to their slower electromagnetic counterparts. Indeed, as far as the S parameters of the radiating mode, S_R, which must be computed by an electromagnetic simulation, do not change—as commented above, they depend mainly of d_1 for a fixed value of d_2 which controls the frequency of the first antenna resonance—, changes in the monopole separation s, which controls the characteristic impedance of the slotline mode, addition of shunt impedances between the monopoles (these affect the slotline mode but not the radiating mode), and changes in the structure of the excitation network can be parametrically analyzed in fast circuit simulations and optimizations.

Using this approach of circuit parametric studies running over a few electromagnetic simulations of the radiating mode, the circuit depicted in Fig. 9 was found to have an excellent capacity for building planar filtennas with a very well-defined radiation band. It consists of the tightly-coupled different-length dipoles of Fig. 1 (with multimodal model given in Fig. 3), fed by a coupled-microstrip section with a gap in one of its strips (Fig. 8(a), with $Z_A = 0$, $Z_B \to \infty$), which is in turn fed by a microstrip line [Fig. 7(a)]. By combining their multimodal circuit models, and removing superfluous 1:1 transformers, a complete multimodal circuit model for the antenna of Fig. 9 can be easily derived, as shown in Fig. 10. Here, the feedback loop through the slotline mode that can modify the radiation behavior of the antenna is apparent, as is the fact that it can be easily controlled by the lengths $d_1 + d_B$ and d_A in the model. Other parameters, such as strip widths and gaps can also control its behavior, though in a more indirect way through their effect on the characteristic impedances of the transmission lines.

6. Filtering antenna design

In order to experimentally validate the filtenna structure and design procedure described above, a filtenna was designed to cover the 3-GHz–5-GHz 5G bands. It was patterned on the Rogers RO4003 substrate considered in Section 4. The antenna was designed by means of circuit parametric simulations using the multimodal circuit of Fig. 10 running over a few electromagnetic simulations of the radiating element (which provided S_R for several d_1 values). The antenna dimensions (see Fig. 9), are $w = 2$ mm, $s = 0.4$ mm, $w_L = 0.6$ mm, $s_L = 0.6$ mm, $d_A = 5.6$ mm, $d_B = 0.5$ mm, $d_1 = 11.3$ mm, $d_2 = 19.1$ mm, ground plane length $d_{GP} = 25$ mm, ground plane width $w_{GP} = 65.1$ mm. The ground-plane edge at the connector side was slotted to increase its impedance to a residual common mode. Fig. 11 shows a top-view picture of the fabricated antenna. The main novelty of the antenna is the addition of dipole-type radiating elements, which allows adding additional resonances to that

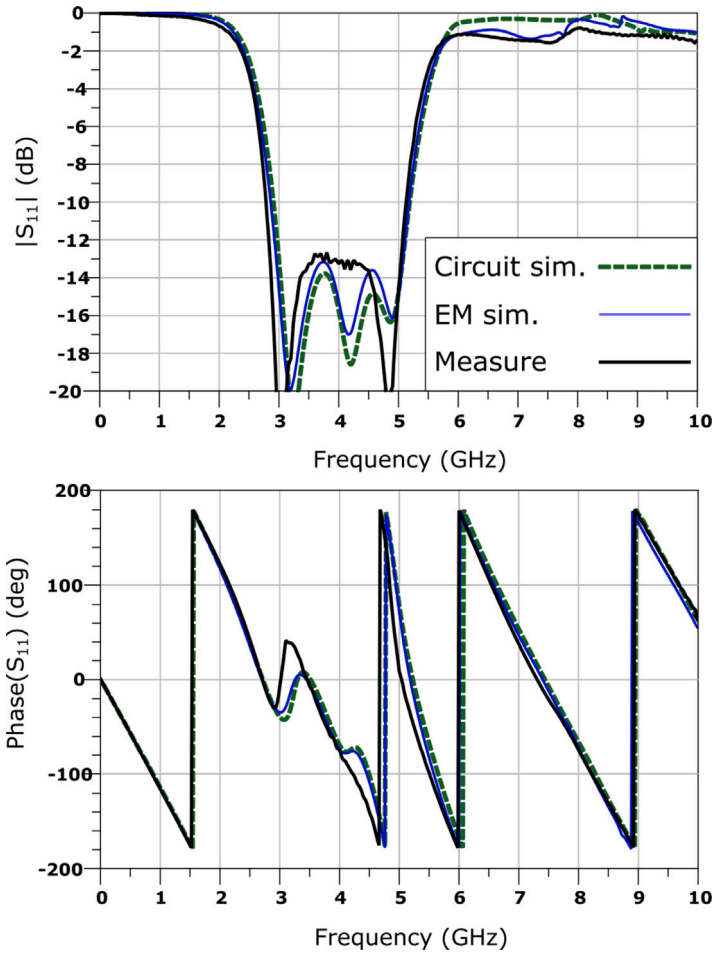

Fig. 12. Simulated (both multimodal-circuit and electromagnetic) and measured S parameters for the radiating element of the antenna.

of the simple monopole which, in combination with a feeding network defining a feedback loop, significantly increases the bandwidth. This concept could be generalized to a larger number of radiating modes.

The measured, Momentum (Keysight™) electromagnetic-simulation and ADS (Keysight™) circuit-simulation—using the multimodal circuit model of Fig. 10 on ADS—reflection coefficient of the antenna is shown in Fig. 12. The antenna exhibits a relative bandwidth of 52% measured at −12 dB (62.9% at −10 dB). The good agreement between measurement and multimodal circuit simulation validates the multimodal circuit model for the antenna of Fig. 10 and proves that multimodal circuit models can be a very useful tool to both understand an antenna behavior and design it. Figs. 13 to 15 compare the simulated and measured radiation diagram and directivity for the antenna at 3.0 GHz, 3.8 GHz (band center) and 5.0 GHz. Finally, the antenna efficiency, measured using the wheeler-cap method, is $\eta = 0.98$ at 3 GHz, $\eta = 0.97$ at 3.8 GHz and $\eta = 0.93$ at 5 GHz.

In Table 1 the performances of the filtenna proposed in this paper (−10-dB FBW, antenna gain and size in terms of the wavelength in vacuum λ_0) are compared to other filtennas of similar central frequencies reported in the literature. It can be observed that the FBW achieved with the proposed multimodal feed (as shown in Fig. 12) is higher than that reported for all other filtennas (except [4]), with the additional advantages of having low complexity and a multimodal feeding structure that integrates both, matching and filtering functions. The gain of the proposed antenna is higher than or comparable to other filtennas with similar dimensions and complexity.

7. Conclusion

In this work, a novel structure for a simple planar filtenna based on two tightly-coupled different-length monopoles is presented and tested. The key to the design and the main novelty of the antenna is the coupling of a monopole to a longer open-circuit radiating element. This coupling, combined with an appropriate feeding network allows a significant increase in bandwidth. It would be possible to increase the number of coupled elements to increase the order of filtering.

First, a multimodal circuit model for the different-length monopoles and their feeding network is derived. It separates the contributions of the radiating and conducting current modes into different ports. In particular, it casts light into the complex interaction between radiation and conduction that takes place at the end of the short monopole, which is used to define a feedback loop capable of improving the antenna bandwidth.

Then, this circuit model is used to design the filtenna using fast parametric circuit simulations running over a few electromagnetic simulations of the more-invariant radiating mode.

The designed planar filtenna features a well-defined 2.8-GHz–5.2-GHz radiation band (−10-dB FWB of 62.9%), with S_{11} better than −12 dB in the 3-GHz–5-GHz band, a gain between 3 dB and 3.5 dB, omnidirectional dipole-like radiation, and good out-of-band rejection up to 10 GHz.

The designed filtenna offers a very good trade-off between structural and design simplicity, and bandwidth, and can be easily integrated on

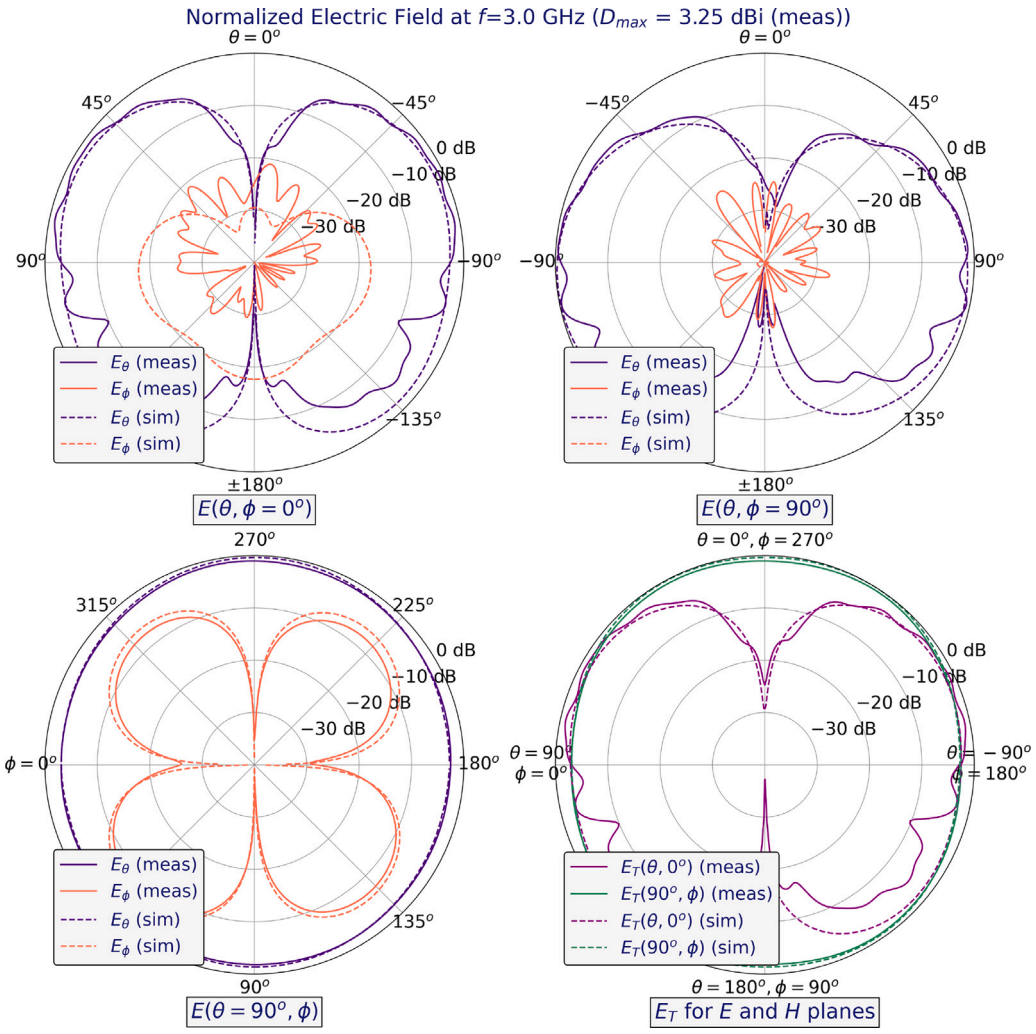

Fig. 13. Radiation parameters at 3.0 GHz: Orthogonal normalized E_θ and E_ϕ cuts, E-plane and H-plane total electric field (E_T), and measured directivity.

Table 1
Comparison with previous filtennas.

Ref	Central frequency (GHz)	Type of filtenna	−10-dB FBW (%)	Gain (dBi) Peak gain (*)	Dimensions (λ_0^2) Estimated (*)	Filtering structure complexity
[4]	6.9	MCR	112.2	2.05–9.8	1.38 × 1.16	Low
[5]	2.45	MCR	9.4	3.3	0.61 × 0.57 (*)	Low
[6]	1.25	MCR	6.32	5.04–6.04	0.5 (*)	Low
[7]	4.8	MCR	35.77	2.25 (*)	0.53 × 0.44	Low
[8]	3.9	MCR	6.4	1.24 (*)	0.65 × 0.65	Low
[9]	3.3/5.76	MCR	42.4/22.6	5.95/4.93 (*)	1.19 × 1.19 (*)	Low
[10]	13.6	SIW	4.1	12.9 (*)	0.88 × 0.88	High
[11]	2.77	SIW	5.1	6.3	0.333	High
[12]	4.42	SIW	6.1	6.7 (*)	0.72 × 0.75 (*)	High
[13]	4.3/5.02	SIW	6	5.94/6.45 (*)	2.27 (*)	High
[15]	6	Multilayer with DR	61.4	8.7	1.2 × 1.2 (*)	High
[16]	2	Two-layer coupled res.	12.8	6.09	0.95 (*)	Very high
[17]	1.7	Multilayer coupled res.	16.9	5.5	0.77 × 0.73 (*)	High
[18]	3.4	Multilayer coupled slots	23.5	6.8	1.13 × 0.37 (*)	High
This work	3.8	Multimodal coupled feed	62.9	3.0–3.5	0.82 × 0.82	Low

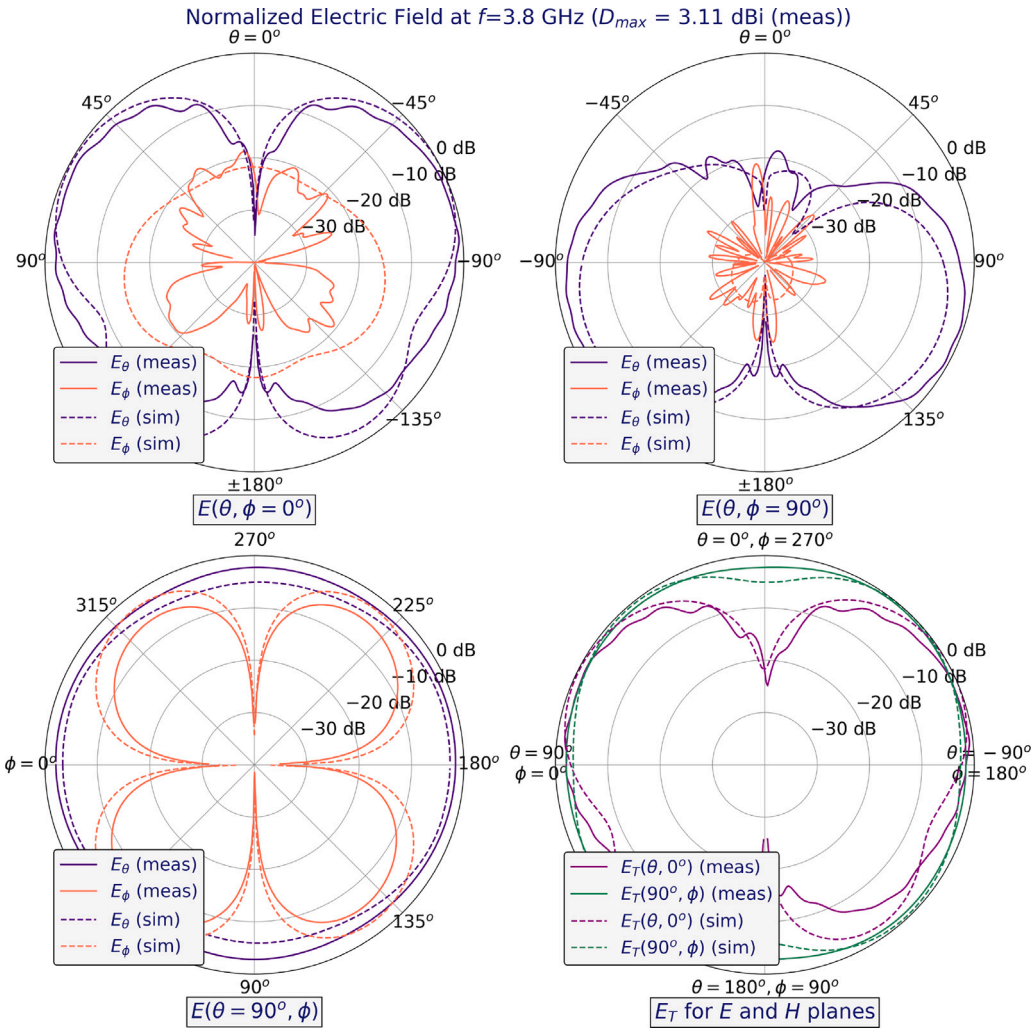

Fig. 14. Radiation parameters at 3.8 GHz: Orthogonal normalized E_θ and E_ϕ cuts, E-plane and H-plane total electric field (E_T), and measured directivity.

the edges of a printed circuit board containing the signal-processing circuitry. The main application of the filtenna is the full coverage of the emerging 5G frequency bands between 3 GHz and 5 GHz (bands n77, n78 and n79).

This work demonstrates how a decomposition of antenna currents into radiating and conducting modes—akin to that used for classic folded dipoles—can be employed to propose new kinds of antennas and to extend the circuit modeling into the antenna bulk. This may be a promising approach to analyze and design other antennas based on two or more coupled monopoles or dipoles.

CRediT authorship contribution statement

Miquel Ribó: Writing – review & editing, Writing – original draft, Visualization, Validation, Supervision, Software, Methodology, Investigation, Formal analysis, Data curation, Conceptualization. **Marta Cabedo-Fabrés:** Writing – review & editing, Writing – original draft, Software, Methodology, Investigation, Formal analysis, Conceptualization. **Lluís Pradell:** Writing – review & editing, Writing – original draft, Validation, Supervision, Resources, Methodology, Investigation, Formal analysis, Conceptualization. **Sebastián Blanch:** Visualization, Software, Resources, Investigation, Data curation. **Miguel Ferrando-Bataller:** Writing – review & editing, Writing – original draft, Validation, Supervision, Software, Resources, Project administration, Methodology, Investigation, Funding acquisition, Formal analysis, Conceptualization.

Declaration of competing interest

The authors declare that they have no known competing financial interests or personal relationships that could have appeared to influence the work reported in this paper.

Data availability

Data will be made available on request.

Acknowledgments

This work was supported in part by Ministerio de Ciencia, Innovación y Universidades, Spain under Grant PID2022-136869NB-C31 financed by MCIN/AEI/10.13039/501100011033/FEDER, UE and PID2022-136869NB-C33 financed by MCIN/AEI/10.13039/501100011033/FEDER, UE.

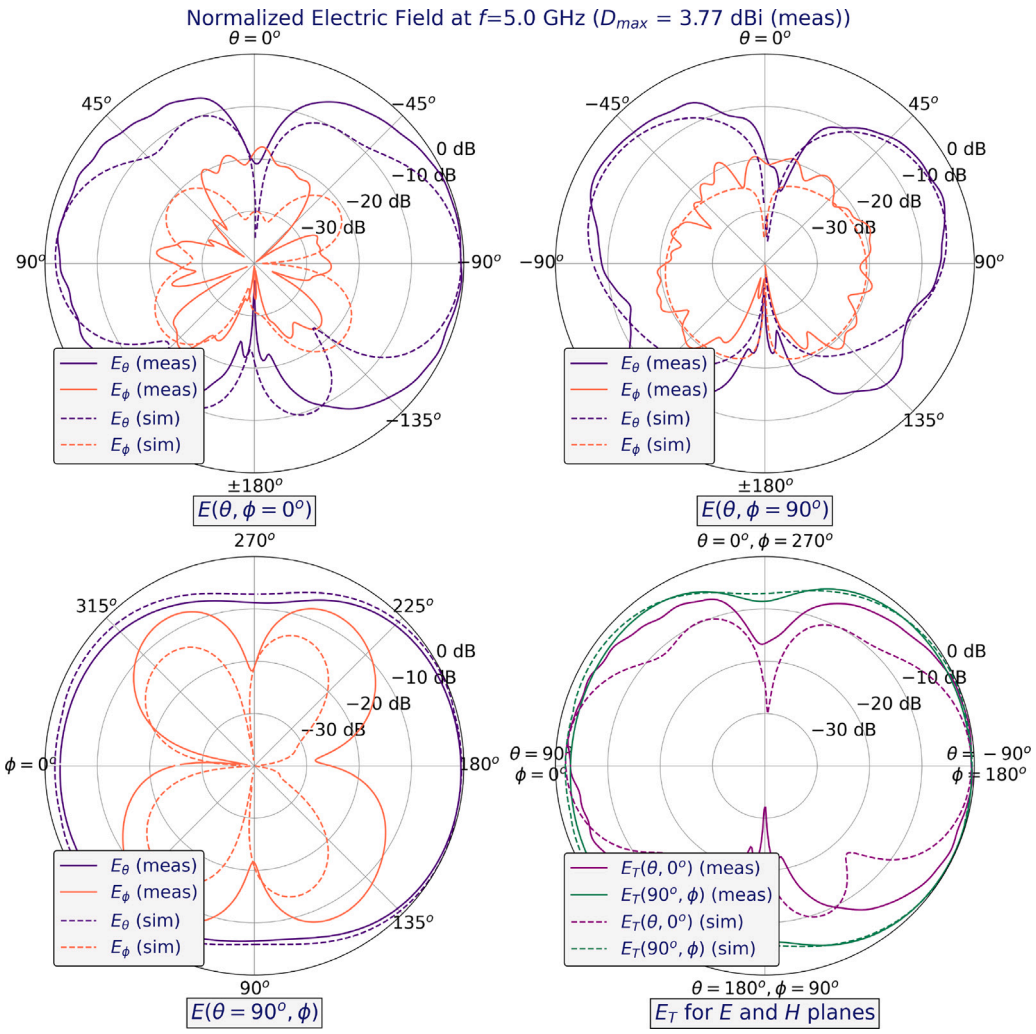

Fig. 15. Radiation parameters at 5.0 GHz: Orthogonal normalized E_θ and E_ϕ cuts, E-plane and H-plane total electric field (E_T), and measured directivity.

References

[1] Shafi M, Molisch AF, Smith PJ, Haustein T, Zhu P, Silva PDe, Tufvesson F, Benjebbour A, Wunder G. 5G: A tutorial overview of standards, trials, challenges, deployment, and practice. IEEE J Sel Areas Commun 2017;35:1201–21. http://dx.doi.org/10.1109/JSAC.2017.2692307.

[2] Shome PP, Khan T, SKoul SK, Antar YMM. Filtenna designs for radio-frequency front-end systems: A structural-oriented review. IEEE Antennas Propag Mag 2021;63:72–84. http://dx.doi.org/10.1109/MAP.2020.2988518.

[3] Mansour G, Lancaster MJ, Hall PS, Gardner P, Nugoolcharoenlap E. Design of filtering microstrip antenna using filter synthesis approach. Prog Electromagn Res 2014;145:59–67. http://dx.doi.org/10.2528/PIER14011405.

[4] Ranjan P, Raj S, Upadhyay G, Tripathi S, Tripathi VS. Circularly slotted flower shaped UWB filtering antenna with high peak gain performance. AEU-Int J Electron Commun 2017;81:209–17. http://dx.doi.org/10.1016/j.aeue.2017.08.055.

[5] Cheng W, Li D. Circularly-polarized filtering monopole antenna based on miniaturized coupled filter. Electron Lett 2017;53:700–2. http://dx.doi.org/10.1049/el.2017.1094.

[6] Tang MC, Chen Y, Shi T, Ziolkowski RW. Bandwidth-enhanced, compact, near-field resonant parasitic filtennas with sharp out-of-band suppression. IEEE Antennas Wirel Propag Lett 2018;17:1483–7. http://dx.doi.org/10.1109/LAWP.2018.2850325.

[7] Pal P, Sinha R, Mahto SK. A compact wideband circularly polarized planar filtenna using synthesis technique for 5 GHz WLAN application. AEU-Int J Electron Commun 2022;148:154180. http://dx.doi.org/10.1016/j.aeue.2022.154180.

[8] Wu Z, Zhang A, Chen J, Lu X, Li J. Co-design of low profile single-fed circularly polarized filtering antenna with high out-of-band rejection. AEU-Int J Electron Commun 2019;102:99–104. http://dx.doi.org/10.1016/j.aeue.2019.01.031.

[9] Turkeli A, Gorur AK, Altuncu Y. A novel dual-wideband four-port MIMO filtenna for sub-6 GHz 5G communication systems. In: 53rd European microwave conference. EUMC, Berlin, Germany; 2023, p. 790–3. http://dx.doi.org/10.23919/EuMC58039.2023.10290702.

[10] Huang Z, Yan YX, Tang SC, Yu W, Chen JX. Substrate-integrated-waveguide-fed slotted patch filtering antenna and array with enhanced selectivity. AEU-Int J Electron Commun 2023;172:154936. http://dx.doi.org/10.1016/j.aeue.2023.154936.

[11] Hu KZ, Tang MC, Li D, Wang Y, Li M. Design of compact, single-layered substrate integrated waveguide filtenna with parasitic patch. IEEE Trans Antennas and Propagation 2020;68:1134–9. http://dx.doi.org/10.1109/TAP.2019.2938574.

[12] Li PK, You CJ, Yu HF, Li X, Yang YW, Deng JH. Codesigned high-efficiency single-layered substrate integrated waveguide filtering antenna with a controllable radiation null. IEEE Antennas Wirel Propag Lett 2018;17:295–8. http://dx.doi.org/10.1109/LAWP.2017.2787541.

[13] Dhwaj K, Tian H, Itoh T. Low-profile dual-band filtering antenna using common planar cavity. IEEE Antennas Wirel Propag Lett 2018;17:1081–4. http://dx.doi.org/10.1109/LAWP.2018.2832631.

[14] Huang YX, Yan YX, Yu W, Qin W, Chen JX. Integration design of millimeter-wave bidirectional endfire filtenna array fed by SIW filtering power divider. IEEE Antennas Wirel Propag Lett 2022;21:1457–61. http://dx.doi.org/10.1109/LAWP.2022.3171526.

[15] Hu PF, Pan YM, Zhang XY, Zheng SY. Broadband filtering dielectric resonator antenna with wide stopband. IEEE Trans Antennas and Propagation 2017;65:2079–84. http://dx.doi.org/10.1109/TAP.2017.2670438.

[16] Tang MC, Guo P, Li D, Hu KZ, Li M, Ziolkowski RW. Vertically polarized, high-performance, electrically small monopole filtennas. IEEE Trans Antennas and Propagation 2022;70:1488–93. http://dx.doi.org/10.1109/TAP.2021.3111331.

[17] Tang H, Chen JX, Chu H, Zhang GQ, Yang YJ, Bao ZH. Integration design of filtering antenna with load-insensitive multilayer balun filter. IEEE Trans Compon Packag Manuf Technol 2016;6:1408–16. http://dx.doi.org/10.1109/TCPMT.2016.2600541.

[18] Li JF, Chen ZN, Wu DL, Zhang G, Wu YJ. Dual-beam filtering patch antennas for wireless communication application. IEEE Trans Antennas and Propagation 2018;66:3730–4. http://dx.doi.org/10.1109/TAP.2018.2835519.

[19] Wu Z, Tang MC, Ziolkowski RW. Broadside radiating, low-profile, electrically small, huygens dipole filtenna. IEEE Antennas Wirel Propag Lett 2022;21:556–60. http://dx.doi.org/10.1109/LAWP.2021.3138404.

[20] Hu KZ, Tang MC, Li M, Ziolkowski RW. Compact, low-profile, bandwidth-enhanced substrate integrated waveguide filtenna. IEEE Antennas Wirel Propag Lett 2018;17:1552–6. http://dx.doi.org/10.1109/LAWP.2018.2854898.

[21] Yan YX, Huang YX, Tang SC, Chen JX. Low-sidelobe microstrip patch filtenna array fed by higher order mode SIW cavity. IEEE Antennas Wirel Propag Lett 2023;22:1873–7. http://dx.doi.org/10.1109/LAWP.2023.3268172.

[22] Scanlan JO. Theory of microwave coupled-line networks. In: Proc IEEE. Vol. 68, 1980, p. 209–31. http://dx.doi.org/10.1109/PROC.1980.11618.

[23] Zysman GI, Johnson AK. Coupled transmission line networks in an inhomogeneous dielectric medium. IEEE Trans Microw Theory Tech 1969;17:753–9. http://dx.doi.org/10.1109/TMTT.1969.1127055.

[24] Tripathi VK. Asymmetric coupled transmission lines in an inhomogeneous medium. IEEE Trans Microw Theory Tech 1975;23:734–9. http://dx.doi.org/10.1109/TMTT.1975.1128665.

[25] Tsai CM, Gupta KC. A generalized model for coupled lines and its applications to two-layer planar circuits. IEEE Trans Microw Theory Tech 1992;40:2190–9. http://dx.doi.org/10.1109/22.179880.

[26] Pajares FJ, Ribó M, Regué JR, Rodríguez-Cepeda P, Pradell L. Circuit models for mode conversion in clock signal distribution. In: Proc 2005 IEEE int symp electromagn compat. Chicago, IL, USA; 2005, p. 39–44. http://dx.doi.org/10.1109/ISEMC.2005.1513468.

[27] Pajares FJ, Ribó M, Regué JR, Rodríguez-Cepeda P, Pradell L. Circuit model for series asymmetric impedances in differential signal paths. In: Proc int symp on electromagn compat – EMC europe 2004. Eindhoven, The Netherlands; 2004, p. 485–8.

[28] Harrington R, Mautz J. Theory of characteristic modes for conducting bodies. IEEE Trans Antennas and Propagation 1971;19:622–8. http://dx.doi.org/10.1109/TAP.1971.1139999.

[29] Cabedo-Fabres M, Antonino-Daviu E, Valero-Nogueira A, Ferrando-Bataller M. The theory of characteristic modes revisited: A contribution to the design of antennas for modern applications. IEEE Antennas Propag Mag 2007;49:52–68. http://dx.doi.org/10.1109/MAP.2007.4395295.

[30] Antonino-Daviu E, Cabedo-Fabrés M, Ferrando-Bataller M, Vila Jimenez A. Active UWB antenna with tunable band-notched behavior. Electron Lett 2007;43(18):959–60. http://dx.doi.org/10.1049/el:20071567.